Cascade-like signal propagation in chains of concave nanomagnets

Cite as: Appl. Phys. Lett. **100**, 152406 (2012); https://doi.org/10.1063/1.3703591
Submitted: 30 January 2012 . Accepted: 27 March 2012 . Published Online: 13 April 2012

Brian Lambson, Zheng Gu, David Carlton, Scott Dhuey, Andreas Scholl, Andrew Doran, Anthony Young, and Jeffrey Bokor

Cascade-like signal propagation in chains of concave nanomagnets

Brian Lambson,[1,a)] Zheng Gu,[1] David Carlton,[1] Scott Dhuey,[2] Andreas Scholl,[3] Andrew Doran,[3] Anthony Young,[3] and Jeffrey Bokor[1]
[1]*Department of Electrical Engineering and Computer Sciences, University of California, Berkeley, California 94720, USA*
[2]*Molecular Foundry, Lawrence Berkeley National Laboratory, Berkeley, California 94720, USA*
[3]*Advanced Light Source, Lawrence Berkeley National Laboratory, Berkeley, California 94720, USA*

(Received 30 January 2012; accepted 27 March 2012; published online 13 April 2012)

We lithographically control the anisotropy properties of single-domain nananomagnets for use in emerging nanomagnetic logic applications. By defining concave-shaped nanomagnets to enhance the effect of configurational anisotropy, we induce the property of dual-axis remanence needed for high-speed and reliable operation of nanomagnetic logic circuits. Magneto-optical measurements verify the anisotropy properties of isolated concave nanomagnets, and photoelectron emission microscopy measurements verify signal propagation in chains of concave nanomagnets. © *2012 American Institute of Physics*. [http://dx.doi.org/10.1063/1.3703591]

Measurement techniques based on the magneto-optical Kerr effect (MOKE) for characterizing anisotropy in single-domain nanomagnets were developed over a decade ago and spurred investigations into the role of a nanomagnet's shape, size, and crystallinity on its anisotropy properties.[1–4] In polygon-shaped nanomagnets, energetically favorable non-uniform magnetization patterns were found to induce "configurational" anisotropy with magnetic easy axes oriented towards either the corners or edges of the polygon, depending on the film thickness. These results hinted at the ability to tune the anisotropy properties of a nanomagnet by changing its lithographically defined shape, which could have broad applicability, for example, to spin-based computation devices.[5,6] However, the relatively small number of adjustable parameters in simple shapes such as rectangles and squares has thus far limited applications of configurational anisotropy.

Configurational anisotropy arises in single-domain nanomagnets that adopt a non-uniform magnetization pattern to minimize magnetic charge at interfaces. The energy landscape in configuration space may contain local minima that do not exist when considering the case of uniform magnetization only, leading to complex anisotropy properties. One way to determine the approximate strength of configurational anisotropy in a particular shape is to associate an effective anisotropy field with each magnetization angle. If the anisotropy is predominantly uniaxial or biaxial, then the difference between the maximum and minimum strength of the anisotropy field is related to the anisotropy energy density K by the equation $H_{anis} = \frac{2K}{M_S}$, where M_S is the saturation magnetization of the material. Past investigations of permalloy squares of 150 nm width and 15 nm thickness have demonstrated a biaxial anisotropy field of over 300 Oe, with easy axes oriented along the square diagonals.[2] Studies have also found that the effect of configuration on magnetic anisotropy is influenced by the presence of geometrical indentations in the nanomagnet shape.[7,8]

One potential application of configurational anisotropy is to nanomagnetic logic, in which arrays of lithographically defined nanomagnets process information via nearest-neighbor dipole coupling interactions.[9–11] Most studies of nanomagnetic logic to date have been carried out using nanomagnets with ellipsoidal or rectangular shapes that are typically assumed to exhibit only uniaxial shape anisotropy. However, a recent simulation study predicts that nanomagnetic logic using nanomagnets with a composition of both uniaxial and biaxial anisotropies could have greatly improved speed and reliability characteristics compared with shape anisotropy only.[12] The study outlines a nanomagnetic logic architecture in which nanomagnets remain magnetized along their shape hard axis until triggered to flip to their shape easy axis by the dipole field their nearest neighbor. The requirement for this architecture to work is that each nanomagnet must exhibit dual-axis remanence (zero-field stability along two orthogonal axes), a property which can be attained by engineering the anisotropy properties of each nanomagnet.

Here, we propose a rectangle-derived nanomagnet shape, which has concavities along its two short edges (top and bottom) to obtain the desired anisotropy properties for nanomagnetic logic applications. As in an elliptical nanomagnet, the shape easy axis lies parallel to the long axis. However, unlike an elliptical nanomagnet, the concavities induce an additional easy axis along what is ordinarily the shape hard axis. To demonstrate this experimentally, we fabricated large (1×1 mm) arrays of nominally identical nanomagnets using electron beam lithography followed by metal evaporation. The center-to-center spacing between nanomagnets is 750 nm. The nanomagnets were defined by electron beam lithography (Vistec VB300 100 kV System) using a silicon substrate and polymethyl-methacrylate (PMMA) resist. After development in a solution of 7:3 isopropanol:water at −5 °C, we deposited a film of 10 nm $Ni_{80}Fe_{20}$/2 nm Al by electron beam evaporation. We then lifted off the pattern using Remover PG. A scanning electron micrograph of a typical finished array is shown in Fig. 1(a).

The anisotropy properties of the finished arrays of nanomagnets were characterized using a MOKE magnetometer configured to perform modulated field magnetic anisometry

a)Electronic mail: lambson@eecs.berkeley.edu.

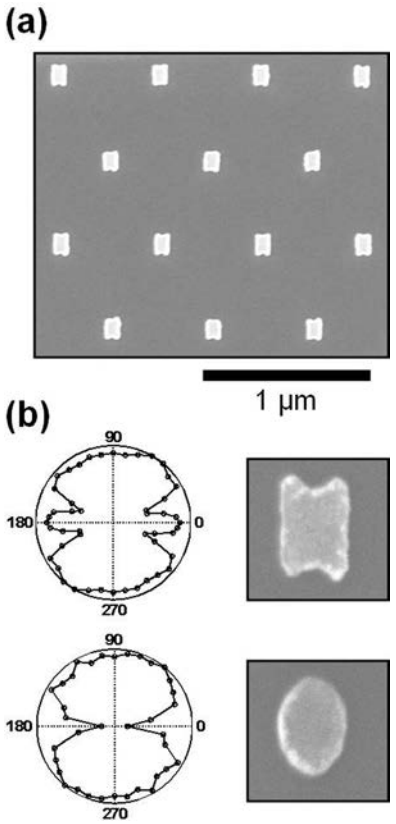

FIG. 1. (a) Scanning electron micrograph of a typical array of nanomagnets used for MFMA measurements. (b) Scanning electron micrographs and corresponding anisotropy profiles of a concave rectangular nanomagnet (top) and elliptical nanomagnet (bottom).

(MFMA) measurements.[1] The measurement yields the angular dependence of the anisotropy strength in the plane of the nanomagnets; maxima in the anisotropy profile indicate magnetic easy axes and minima indicate hard axes. Because configurational anisotropy depends on the non-uniform magnetization of the nanomagnets and requires each spin to be treated as an independent variable, quantifying cubic and uniaxial anisotropy parameters, as is done for uniformly magnetized particles, is not possible. In Fig. 1(b), we compare the experimental anisotropy profile of a permalloy concave rectangle with that of an ellipse. The nominal dimensions of the nanomagnets are 80 nm × 120 nm with a 10 nm thickness. In both ellipses and concave rectangles, we clearly observe a dominant shape easy axis in the vertical direction, but only in the concave rectangle do we additionally observe a minor easy axis in the horizontal direction. Next, we measured hysteresis loops along the hard (short) axis of the nanomagnets, shown in Fig. 2, as well as along the easy (long) axis of the nanomagnets by MOKE magnetometry. Unlike ellipsoidal nanomagnets, concave rectangles exhibit hysteresis along their shape hard axis, while both exhibit hysteresis along their shape easy axis. The observation of dual-axis remanence implies that the anisotropy energy barriers that separate the two stable axes are significantly larger than the thermal energy, kT, at room temperature.

Information in a nanomagnetic logic circuit with dual-axis remanence is predicted to propagate in a characteristic cascade-like manner.[12] Using micromagnetic simulations,[13] we verify that this mode of signal propagation occurs in

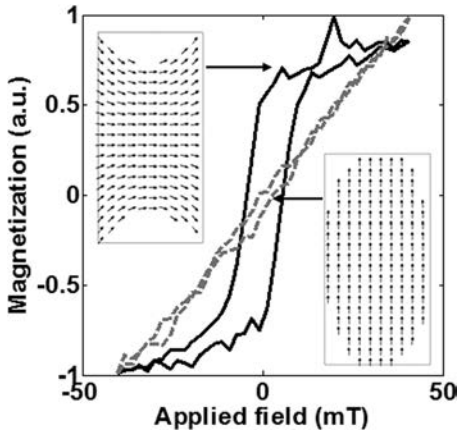

FIG. 2. Comparison of hysteresis loops measured along the hard axis of concave and ellipsoidal nanomagnets by MOKE magnetometry. Micromagnetic simulations (inset) show the remanent configuration of each shape.

chains of concave nanomagnets, as shown in Fig. 3(a). For comparison, we also simulated a chain of elliptical nanomagnets with equivalent dimensions. In both simulations, the leftmost magnet is fixed in the vertical direction to set the desired output state of the chain, and the rightmost magnet is fixed to the right to stabilize the terminal magnet. The nanomagnets are initialized along the horizontal axis by an applied magnetic field of 150 mT, which is removed linearly over the first 1 ns of simulation time to initialize signal propagation. The temperature parameter in the simulations is set to 300 K. Each concave nanomagnet remains magnetized in its metastable state along the horizontal axis until its nearest neighbor flips and produces a dipole field in the vertical direction, giving rise to the predicted cascade-like behavior. By contrast, in the ellipsoidal chains, stochastic thermal processes caused the nanomagnets to flip to the vertical axis too rapidly for the information from the input magnet to propagate reliably down the chain. As a result, some of the magnets flip to a logically incorrect state (parallel to their nearest neighbors). Simulations carried out using nanomagnets with different concavity shapes, e.g., with rounded rather than pointed ends, exhibited similar cascade-like signal propagation behavior.

Photoelectron emission microscopy (PEEM) experiments were carried out at the Advanced Light Source, Lawrence Berkeley National Laboratory to verify the unique behavior of chains of concave nanomagnets. Magnetic circular dichroism of circularly polarized x-rays was used to generate magnetic contrast images with sensitivity along the shape easy axes of the nanomagnets. In Fig. 3(b), a scanning electron micrograph of a typical chain of concave nanomagnets under investigation is shown. The nanomagnet dimensions are 80 nm × 160 nm with 10 nm thickness. The concavity depth was varied between 20 and 40 nm. Prior to magnetic imaging, a 220 mT magnetic field was applied along the horizontal axis of the chain and subsequently removed over 30 s. The sample was then inserted into the PEEM chamber and magnetic contrast images were taken. The bottom image in Fig. 3(b) suggests that nanomagnets with 20 nm concavity depth were not sufficiently stabilized along the horizontal axis by biaxial anisotropy; all the nanomagnets flip to the vertical axis, but errors (nearest neighbors

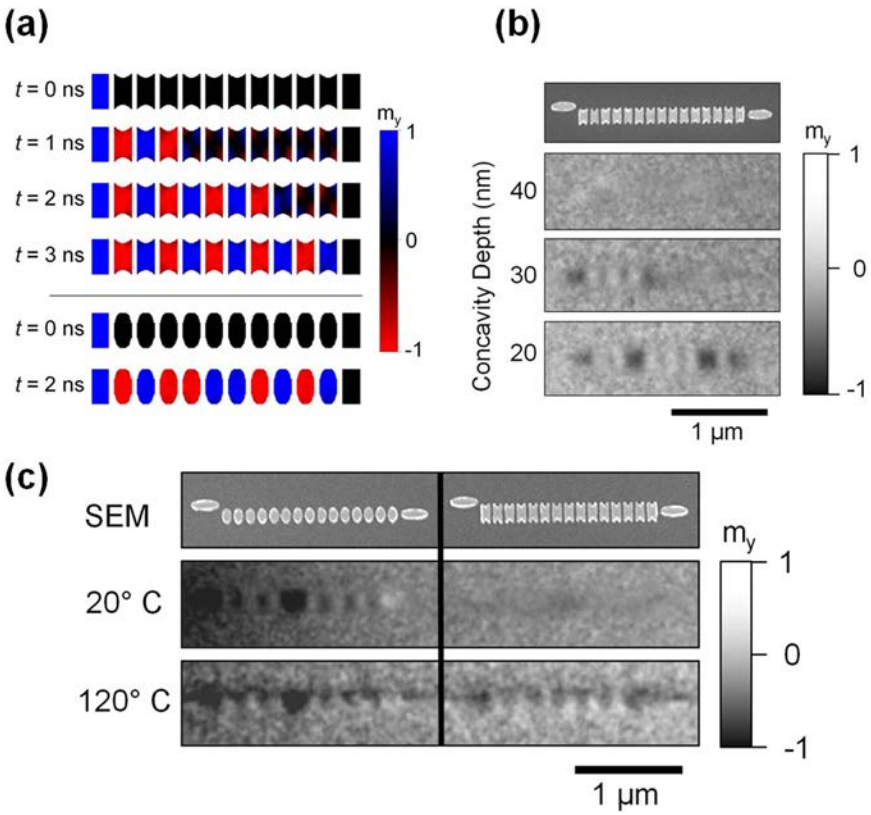

FIG. 3. (a) Micromagnetic simulations showing cascade-like signal propagation in a chain of concave nanomagnets (top) and error-prone signal propagation in a chain of elliptical nanomagnets (bottom). (b) Scanning electron micrograph and magnetic contrast images of chains of concave nanomagnets with varying concavity depths. The nanomagnet dimensions are 80 nm × 160 nm. (c) Scanning electron micrograph and magnetic contrast images of chains of elliptical (left) and concave (right) nanomagnets at varying temperatures. The nanomagnet dimensions are 80 nm × 154 nm, with 30 nm concavity depth.

aligned parallel to one another) are observed in the output state of the chain. On the other hand, nanomagnets with 40 nm concavity depth did not flip to the vertical axis at all (the lack of magnetic contrast indicates horizontal magnetization). This implies that the biaxial anisotropy was strong relative to the uniaxial anisotropy, so the magnets remained locked in the horizontal direction. Finally, nanomagnets with 30 nm concavity depth demonstrate an appropriate balance of biaxial and uniaxial anisotropy, as error-free signal propagation occurs along the first seven nanomagnets in the chain.

Further confirmation of the intended behavior of concave nanomagnets was achieved by increasing the temperature of the nanomagnet chains while inside the PEEM chamber. In Fig. 3(c), we first show scanning electron micrographs of two neighboring chains in which the left chain consists of elliptical nanomagnets and the right chain consists of concave nanomagnets. Next, we show a magnetic contrast image of the two chains taken at room temperature. The chain of elliptical nanomagnets does not exhibit metastability and is magnetized along the vertical axis, while the chain of concave nanomagnets is magnetized along the horizontal axis. Then, to verify that the horizontal magnetization of the concave nanomagnet chain is a metastable state—rather than a global energy minimum—we raised the temperature of the sample to 120 °C using a heating filament inside the sample stage. The increase in thermal energy allows the nanomagnets to hop over the biaxial anisotropy energy barriers and permanently flip out of the metastable state. The final magnetic contrast image shown in Fig. 3(c) confirms that the heated chain no longer remains locked along the horizontal axis and instead flips to the vertical axis, with anti-parallel nearest-neighbor alignment.

This report demonstrates the use of concave shapes to achieve tunable control of the anisotropy properties of nanomagnets for nanomagnetic logic applications. One of its key advantages over other means of anisotropy control is that it is induced by top-down lithography and can be fabricated using well-characterized processes like permalloy lift-off. Further exploration of the nanomagnet shape space in search of useful anisotropy properties will be fruitful for additional nanomagnetic applications.

This work was supported in part by the DARPA Non-Volatile Logic Program, the Western Institute of Nanoelectronics (WIN) and the Center for Energy Efficient Electronics Sciences (NSF Award Number ECCS-0939514). Work at the Molecular Foundry and the Advanced Light Source, Lawrence Berkeley National Laboratory was supported by the Director, Office of Science, Office of Basic Energy Sciences, Division of Materials Sciences and Engineering of the US Department of Energy under Contract No. DE-AC02-05CH11231.

[1]R. P. Cowburn, A. Ercole, S. J. Gray, and J. A. C. Bland, "A new technique for measuring magnetic anisotropies in thin and ultrathin films by magneto-optics," J. Appl. Phys. **81**, 6879 (1997).
[2]R. P. Cowburn, A. O. Adeyeye, and M. E. Welland, "Configurational anisotropy in nanomagnets," Phys. Rev. Lett. **81**, 5414 (1998).
[3]P. Vavassori, D. Bisero, F. Carace, A. di Bona, G. C. Gazzadi, M. Liberati, and S. Valeri, "Interplay between magnetocrystalline and configurational anisotropies in Fe(001) square nanostructures," Phys. Rev. B **72**, 054405 (2005).
[4]R. P. Cowburn, "Property variation with shape in magnetic nanoelements," J. Phys. D: Appl. Phys. **33**, R1 (2000).
[5]B. Behin-Aein, D. Datta, S. Salahuddin, and S. Datta, Nat. Nanotechnol. **5**, 266 (2010).
[6]S. S. P. Parkin, M. Hayashi, and L. Thomas, "Magnetic domain-wall racetrack memory," Science **320**, 190 (2008).
[7]D. K. Koltsov and M. E. Welland, "Control of micromagnetics in permalloy nanomagnets by means of indentation," J. Appl. Phys. **94**, 3457 (2003).

[8]F. Lee, "Shape-induced biaxial anisotropy in thin magnectic films," IEEE Trans. Magn. **4**, 502 (1968).
[9]A. Imre, G. Csaba, L. Ji, A. Orlov, G. H. Bernstein, and W. Porod, "Majority logic gate for magnetic quantum-dot cellular automata," Science **311**, 205 (2006).
[10]B. Lambson, D. Carlton, and J. Bokor, "Exploring the thermodynamic limits of computation in integrated systems: Magnetic memory, nanomagnetic logic, and the landauer limit," Phys. Rev. Lett. **107**, 010604 (2011).
[11]D. Carlton, B. Lambson, A. Scholl, A. Young, P. Ashby, S. Dhuey, E. Tuchfeld, and J. Bokor, "Computing in thermal equilibrium with dipole-coupled nanomagnets," IEEE Trans. Nanotechnol. **10**, 1401 (2011).
[12]D. B. Carlton, N. C. Emley, E. Tuchfeld, and J. Bokor, "Simulation studies of nanomagnet-based logic architecture," Nano Lett. **8**, 4173 (2008).
[13]M. Donahue and D. Porter, "OOMMF User's Guide, Version 1.0," Interagency Report NISTIR 6376 (National Institute of Standards and Technology, Gaithersburg, MD, 1999). http://math.nist.gov/oommf/.